ISSN 1064-2293, Eurasian Soil Science, 2020, Vol. 53, No. 9, pp. 1195–1205. © Pleiades Publishing, Ltd., 2020.
Russian Text © The Author(s), 2020, published in Pochvovedenie, 2020, No. 9, pp. 1041–1052.

GENESIS AND GEOGRAPHY OF SOILS

Influence of Forest Shelterbelts on Local Pedodiversity (Belgorod Oblast)

M. A. Smirnova[a], *, A. N. Gennadiev[a], Yu. G. Chendev[b], and R. G. Kovach[a]

[a] *Lomonosov Moscow State University, Moscow, 119991 Russia*
[b] *Belgorod State University, Belgorod, 308015 Russia*
**e-mail: summerija@yandex.ru*

Received March 10, 2020; revised March 15, 2020; accepted April 1, 2020

Abstract—Detailed mapping of soils under a multi-row 4-km-long 50-year-old forest shelterbelt crossing diverse landforms and under adjacent croplands was performed at the key site in Belgorod oblast, in the south of the Central Russian Upland. Samples were collected in 30 points both in the central part of the shelterbelt and at distances of 30 meters on both sides of the shelterbelt. Maps of the depth of humus horizon, organic carbon content, depth of carbonates, and the soil map were compiled; indices of richness, diversity (Shannon, Simpson, Rao) and taxonomic distances (as a quantitative indicator of soil cover contrasts) were calculated. It was shown that soils under the shelterbelt are less contrasting among one another and more diverse than soils of the adjacent croplands. The shelterbelt effect on pedodiversity at the key site extends over adjacent areas affected by periodic waterlogging due to the barrier function of the shelterbelt.

Keywords: soil cover pattern, Central Russian Upland, pedodiversity, Chernozems, taxonomic distance
DOI: 10.1134/S1064229320090161

INTRODUCTION

Since 1948, as a result of the implementation of state programs of agroforestry in Russia, a large number of field-protective forest shelterbelts have been planted; at present, their age reaches 50–70 years. In the course of their functioning, forest shelterbelts have influenced the quality of soils. Studies of the results of this influence were performed by many researchers, mainly from the point of view of the significance of shelterbelts for increasing soil fertility. The published works dealt mainly with the applied aspects of evaluating field-protective forest shelterbelts as the factors that (a) increase crop productivity via improving the water balance, (b) reduce the intensity of soil erosion under the influence of the barrier role of shelterbelts, (c) contribute to carbon dioxide sequestration thus reducing the greenhouse effect, etc. [1, 4, 8, 10, 12, 14, 16, 21, 24]. At the same time, forest shelterbelts were also considered as original objects of experimental transformation of soil formation conditions, which made it possible to expand and deepen the fundamental evolutionary-genetic concepts of soils and soil cover. In particular, the shelterbelt–soil system can act as a controlled model of the development of pedodiversity, the parameters of which are set in the spatiotemporal dimension. In recent years, more attention has been paid pedodiversity; this phenomenon is considered at various spatial scales: global, continental, regional [3, 7, 15, 18–20, 23, 25, 27]. The study of the shelterbelt–soil system makes it possible to quantitatively characterize the transformation of the soil cover and link it to the timescale; in particular, the changes in pedodiversity under the influence of a factor external to the soils at the local level can be traced. This was the main purpose of our study.

OBJECTS AND METHODS

Field studies were carried out in the forest-steppe zone of the south of the Central Russian Upland, at the Stepnoe key site (Fig. 1) located in Gubkin district of Belgorod oblast, in the vicinity of the village of Stepnoe (coordinates of the center of the shelterbelt: 50.9988° N, 37.3378° E). According to the nearest weather station data in Bogoroditskoe, 18 km north of the key site, this territory has a moderately continental climate with the mean annual temperature +7.5°C and mean annual precipitation 558 mm (for the period from 2015 to 2019).

The key site includes a part of a long multi-row forest shelterbelt and adjacent agricultural fields. The size of the site is 500 × 4000 m. The shelterbelt is shown on a large-scale topographic map dated back to 1981. According to this mapt, the shelterbelt consists of maple and ash trees, the height of which reaches 5 m in the northern part and 8 m in the southern part. The trees reach this height in 10–15 years. Hence, at present, the age of the shelterbelt is about 50–55 years.

Fig. 1. Fragment of a satellite image of the key site and location of soil sampling points.

Crop rotations practiced on agricultural fields adjacent to the shelterbelt mainly include grain crops. Traditional moldboard plowing to a depth of 25–30 cm is applied on these fields [5].

The shelterbelt extends from the south to the north crosses various elements of the local topography, including the watershed surface, gentle and steep slopes of northern and southern aspects, and bottoms of the hollows; the amplitude of heights between these geomorphic positions at the key site as about 5 m (Fig. 2). The surface of the site is slightly inclined to the west. As a result, water stagnation and ponding may take place in spring in the upper reaches of the hollow crossed by the shelterbelt and found to the east of it (Fig. 3). The degree of relief dissection also increases in the same direction.

Ten parallel transects were laid perpendicular to the shelterbelt. Each of them included three sampling points (Fig. 1): in the axial part of the shelterbelt (the width of the shelterbelt is from 30 to 50 m) (indicated by letter S) and at distances of 30 m from the western and eastern edges of the shelterbelt on agricultural fields that are denoted as west field (W) and east field (E). At each point, the description of topography and vegetation was performed, and soil pits (transects 7 and 9) or boreholes (transects 1–6, 8, and 10) to a depth of more than 1.2 m were examined. Classification and diagnostics of soils was carried out in accordance with the *Classification and Diagnostics System for Russian Soils* [6].

The number of rows in the studied shelterbelt varies from 5 to 12. The species composition is heterogeneous. In the southern part of the studied site (transects 1–3), ash is the main tree species; maple is also present. The height of the trees is 20–25 m, the diameter of the trunks is up to 35 cm. The number of rows varies from 10 to 12. In the undergrowth, there are cotoneaster (*Cotoneaster*) and common robinia (*Robinia pseudoacacia*) shrubs. The herbaceous cover is developed fragmentarily; the degree of projective cover does not exceed 10–15%. The soil surface is densely covered with leaf litter of the past year; there are large branches and tree trunks. In the area between transects 3 and 4, the trees are absent (no trees were planted). The section of the shelterbelt crossed by transect 4 is sparse and consists of five rows of birch trees. The height of the trees does not exceed 25 m, the diameter of the trunks is up to 30 cm. The degree of projective cover of the herbaceous layer is less than 30%. In the central and northern parts of the shelterbelt (transects 5–10), the tree layer is represented by maple, birch, and pear. The number of rows varies from eight to twelve. The height of the trees does not exceed 25 m, the diameter of the trunks is less than 45 cm.

Two-layered sediments serve as parent material. The upper layer is represented by calcareous loesslike loam, and the underlying layer is carbonate-free clay. The thickness of the upper layer within the study area varies from 60 cm to more than two meters. The underlying clayey layer at a depth of less than 1 m was described in pits 7E, 2W, and 3W; at a depth from 1 to 1.5 meters, in pits 3E, 4E, 4S, 7S, 7W, and 8E. In other pits, it was more than two meters. The changes in thickness of the upper loamy layer do not display definite agreement with the surface topography.

To determine the content of organic carbon at the sampling points, soil samples were taken from the plow layer of 0–30 cm in the fields and from the depths of 0–10, 10–20, and 20–30 cm under the shelterbelt. In the soils confined to the watershed surface (transect 9) and to the bottom of the hollow (transect 7), additional samples were taken from all genetic horizons. The CO_2 of carbonates was determined in the samples from the carbonate horizons. They were differentiated into two parts: the upper part, where the soil effervesces with 10% HCl, but does not contain morphologically distinct carbonate concentrations (pedofeatures), and the lower part with distinct carbonate concentrations. The content of carbonates was separately determined in both parts, Overall, 95 sam-

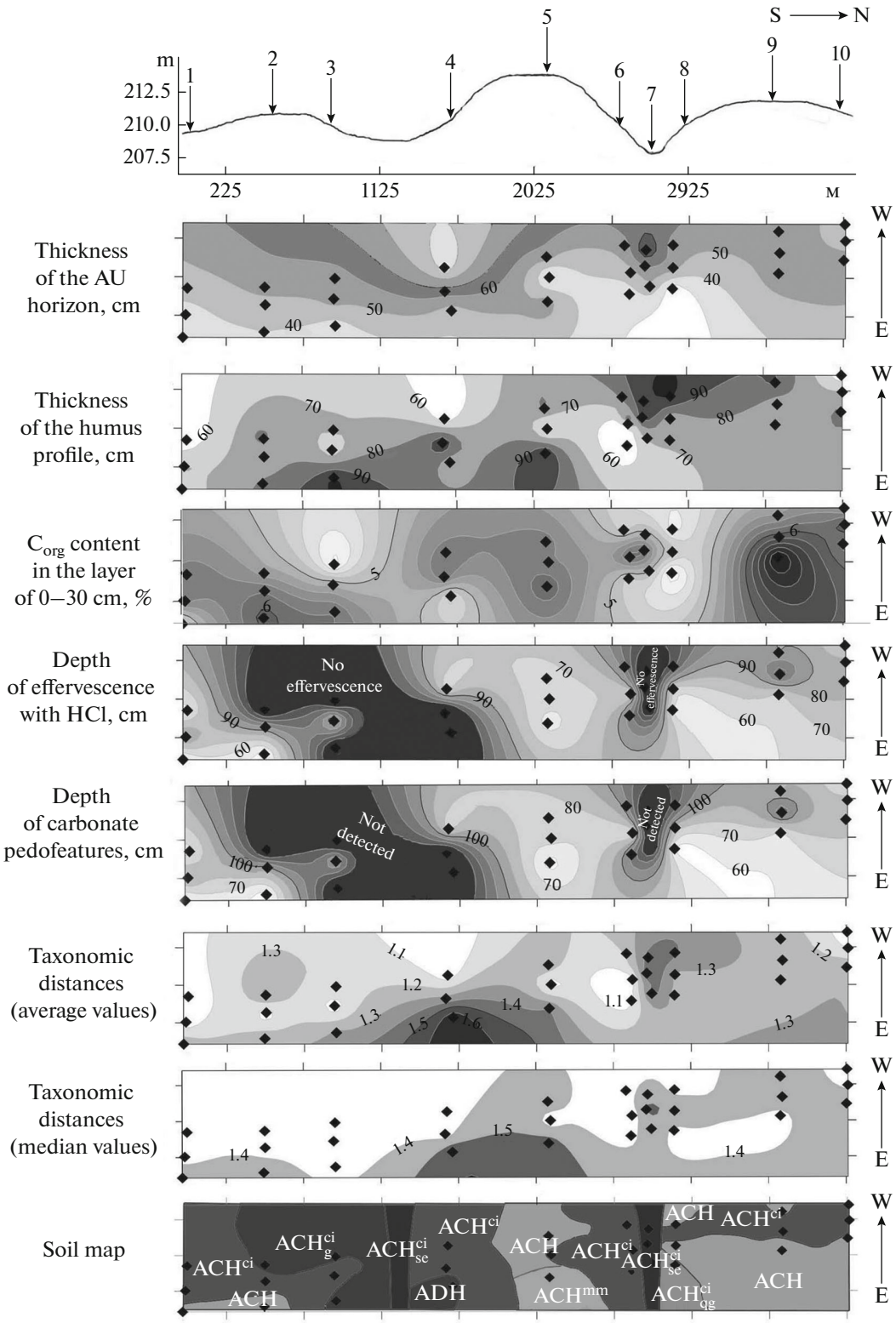

Fig. 2. Schematic profile across the key site with indication of the numbers of studied transects, the maps of soil properties, and the soil map of the key site. Soil codes: ACH—mycellary agrochernozems, ACH^{mm}—migrational–mycellary agrochernozems, ACH^{ci}—clay-illuvial agrochernozems, ACH_{se}^{ci}—stratified eluviated clay-illuvial agrochernozems, ACH_{qg}^{ci}—deeply quasigleyed clay-illuvial agrochernozems, ACH_{g}^{ci}—deeply gleyic clay-illuvial agrochernozems, and ADH—eluviated deeply gleyic agro-dark-humus soils.

Fig. 3. Fragment of the shelterbelt and adjacent east field. Photo taken in May 2019.

Diagnostic indicators		1E	2E	3E	4E	5E	6E	7E	8E	9E	10E	1	2S	3S	4S	5S	6S	7S	8S	9S	10S	1W	2W	3W	4W	5W	6W	7W	8W	9W	10W
Type level	PU	1	1	1	1	1	1	1	1	1	1	1	1	1	1	1	1	1	1	1	1	1	1	1	1	1	1	1	1	1	1
	AU	1	1	1	1	1	1	1	1	1	1	1	1	1	1	1	1	1	1	1	1	1	1	1	1	1	1	1	1	1	1
	BI	0	0	1	0	0	1	1	1	0	0	1	1	1	1	1	1	1	0	1	1	1	1	1	1	0	1	1	0	0	1
	BCA	1	1	0	0	1	1	0	0	1	1	1	1	1	0	1	1	0	1	1	1	1	0	0	1	1	1	0	1	1	1
Subtype level	rh	0	0	0	0	0	0	0.5	0	0	0	0	0	0	0	0	0	0.5	0	0	0	0	0	0	0	0	0	0.5	0	0	0
	el	0	0	0	0.5	0	0	0.5	0	0	0	0	0	0	0	0	0	0.5	0	0	0	0	0	0	0	0	0	0.5	0	0	0
	lc	0	0	0	0	0.5	0	0	0	0	0	0	0	0	0	0	0	0	0	0	0	0	0	0	0	0	0	0	0	0	0
	me	0.5	0.5	0	0	0.5	0.5	0	0	0.5	0.5	0.5	0.5	0.5	0	0.5	0.5	0	0.5	0.5	0.5	0.5	0	0	0.5	0.5	0.5	0	0.5	0.5	0.5
	q	0	0	0	0	0	0	0	0.5	0	0	0	0	0	0	0	0	0	0	0	0	0	0	0	0	0	0	0	0	0	0
	g	0	0	0.5	0.5	0	0	0	0	0	0	0	0	0	0.5	0	0	0.5	0	0	0	0	0.5	0.5	0	0	0	0.5	0	0	0
Genus level	Contrasting deposits	0	0	0.3	0.3	0	0	0.3	0.3	0	0	0	0	0	0.3	0	0	0.3	0	0	0	0	0.3	0.3	0	0	0	0.3	0	0	0
Species level: Thickness of humus horizon	Deep	0	0	0.2	0.2	0.2	0	0.2	0.2	0	0.2	0	0	0	0.2	0	0.2	0.2	0	0	0	0	0.2	0	0	0.2	0.2	0.2	0	0	0
	Medium-deep	0.2	0.2	0	0	0	0.2	0	0	0.2	0	0.2	0.2	0.2	0	0.2	0	0	0.2	0.2	0.2	0.2	0	0.2	0.2	0	0	0	0.2	0.2	0.2
Species level: Humus content	Medium-humus	0	0	0	0	0	0	0	0	0	0	0	0	0	0	0	0	0	0.2	0.2	0.2	0	0	0	0	0	0	0	0	0	0
	Low-humus	0	0.2	0.2	0	0.2	0	0	0	0	0.2	0.2	0.2	0.2	0.2	0.2	0.2	0.2	0	0	0	0.2	0.2	0	0.2	0.2	0	0	0	0.2	0.2
	Weakly humified	0.2	0	0	0.2	0	0.2	0.2	0.2	0.2	0	0	0	0	0	0	0	0	0	0	0	0	0	0.2	0	0	0.2	0.2	0.2	0	0
Species level: Depth of effervescence	Shallow-calcareous	0	0	0	0	0	0	0	0	0	0	0	0	0	0	0	0	0	0	0	0	0	0	0	0	0	0	0	0	0	0
	Medium-deep-calcareous	0.2	0.2	0	0	0.2	0	0	0	0.2	0.2	0	0	0.2	0	0.2	0	0	0.2	0	0.2	0.2	0	0	0.2	0.2	0	0	0.2	0.2	0.2
	deep-calcareous	0	0	0	0	0	0.2	0	0.2	0	0	0.2	0.2	0	0	0	0.2	0	0	0.2	0	0	0	0	0	0	0.2	0	0	0	0

Fig. 4. Matrix table of soil properties; PU, AU, BI, and BCA are soil horizons; 1E, 2E, 3E... 10W are numbers of soil pits.

ples were analyzed for the organic carbon content, and 33 samples were analyzed for the content of carbon dioxide of carbonates.

To assess the degree of contrast in the soil cover, the method for calculating taxonomic distances was used, which was described in detail in [9, 23]. At the first stage, a matrix of soil properties was created (Fig. 4), where the rows corresponded to the soil properties, and the columns corresponded to the studied soils. In each cell of the matrix, the presence (from 0.2 to 1) or absence (0) of a given property (indicator) in the soil was noted. Taxonomically significant characteristics of soil profiles were used as properties, and their weight was assigned in accordance with the hierarchical classification system:

(1) Diagnostic horizons PU, AU, BI, and BCA (independently from the presence or absence of some other diagnostic features in them); weight, 1;

(2) Diagnostic genetic features rh, el, lc, mc, q, g (without their allocation to the particular genetic horizons); weight, 0.5;

(3) Grades of soil characteristics applied at the level of soil genera and the contrasting (two-layered) nature of the parent material; weight, 0.3;

(4) Grades of soil characteristics applied at the species level—the thickness of humus horizon (medium-

deep (50–80 cm) and deep (80–120 cm) chernozems); the content of humus in the topsoil (medium-humus (6–9%), low-humus (4–6%), and weakly humified (<4%) chernozems); and the depth of effervescence (shallow-calcareous (30–50 cm), medium-deep-calcareous (50–80 cm), and deep-calcareous (80–120 cm) chernozems); weight, 0.2.

In total, information was used on the presence or absence of 19 indicators, combinations of which form all the studied soils of the site. It was assumed that the set of indicators entered in the table adequately describes the soils of the key site. The calculation of the taxonomic distance between soils was carried out according to equation (1) [22]:

$$d_{ij} = \sqrt{(x_i - x_j)^T (x_i - x_j)}, \quad (1)$$

where d_{ij} is the taxonomic distance between soils i and j, x_i and x_j are vectors (columns) of the matrix of soil properties. The degree of contrast between soils (relative to one another) is considered to be directly proportional to the values of the taxonomic distance. The maximum taxonomic distance is determined by the number of diagnostic soil properties in the matrix and by the scores assigned to them for their presence or absence in the soil. In our case, the maximum possible value of the taxonomic distance is 2.98. The calculation of taxonomic distances was carried out for several different soil samples: for samples including only east-field soils (that is, only 10 soils), only shelterbelt soils (10 soils), only west-field soils (10 soils); for samples characterizing various elements of the relief: watershed surface and gentle slopes (15 soils), soils of steep slopes (12 soils), and the bottom of a hollow (3 soils); finally, this calculation was performed for the total sample that included all 30 studied soils. For each statistical sample, the average, median, and maximum values of taxonomic distances were determined.

Statistical processing of the results and plotting of the maps were performed with the use of Statistica, QGIS, and Surfer software. The maps of the thickness of the humus horizon, the humus profile, the content of C_{org}, the depth of effervescence, the depth of the appearance of secondary carbonate concentrations, and the map of taxonomic distances were constructed using the ordinary kriging method. The soil map was developed using the expert method described in [11].

A quantitative assessment of pedodiversity was carried out for the soil cover of the shelterbelt, west field, and east field. The criteria were the number of soil taxa forming the soil cover (richness index), the Shannon (2) and Simpson (3) diversity indices, and Rao's square entropy (4), calculated according to the formulas [20, 26]:

$$H = -\sum_{i=1}^{c} p_i \ln p_i, \quad (2)$$

$$G = 1 - \sum_{i=1}^{c} p_i^2, \quad (3)$$

$$Q = \sum_{i=1}^{c} \sum_{j=1}^{c} d_{ij} p_i p_j, \quad (4)$$

where p_i and p_j are the parts of the area occupied by soils i and j in the total soil cover of the plot, c is the number of soil taxa at n the key plot, and d_{ij} is the taxonomic distance between soils i and j.

The Shannon and Simpson diversity indices take into account the component composition and the share of components in the composition of the soil cover; the greater the number of components composing the soil cover, and the closer the sizes of soil areas, the higher the value of the index [20].

The Rao square entropy index, in addition to the share and the number of components, takes into account the degree of contrast between the components in relation to one another [26]. The values of taxonomic distances were used as a parameter of the contrast. With the same number of components and the same share occupied by them in the composition of the soil cover, the diversity is higher, where the degree of contrast between the components in relation to one another is higher.

RESULTS AND DISCUSSION

The soil cover of the key site is characterized by a wide range of soils: three types of soils, seven subtypes, and eighteen species. The following soil species were identified: medium-deep low-humus medium-deep-calcareous clay-illuvial agrochernozems (Luvic Chernozems (Loamic, Aric, Pachic)) (soil profiles 1W, 4W, 10W, 3S, and 5S); medium-deep weakly humified medium-deep-calcareous mycellar agrochernozems (Haplic Chernozems (Loamic, Aric, Pachic) (profiles 1E, 9E, and 8W); deep low-humus deeply gleyic clay-illuvial agrochernozems on contrasting (two-layered) parent material (Luvic Stagnic Chernic Phaeozems (Loamic, Aric, Pachic)) (profiles 3E, 4S, and 2W); deep low-humus medium-deep-calcareous mycellar agrochernozems (Haplic Chernozems (Loamic, Aric, Pachic)) (profiles 10E and 5W), medium-deep low-humus deep-calcareous clay-illuvial agrochernozems (Luvic Chernic Phaeozems (Loamic, Aric, Pachic)) (profiles 1S and 2S); deep weakly humified stratified eluviated deeply gleyic clay-illuvial agrochernozems on contrasting parent material (Luvic Greyzemic Stagnic Chernic Phaeozems (Loamic, Aric, Novic, Pachic)) (profiles 7E and 7W); medium-deep low-humus medium-deep-calcareous mycellar agrochernozems (Haplic Chernozem (Loamic, Aric, Pachic)) (profiles 2E and 9W); deep weakly humified deeply gleyic eluviated agro-dark-humus soil on contrasting parent material (Greyzemic Stagnic Chernic Phaeozem (Loamic, Aric, Pachic)) (profile 4E); deep

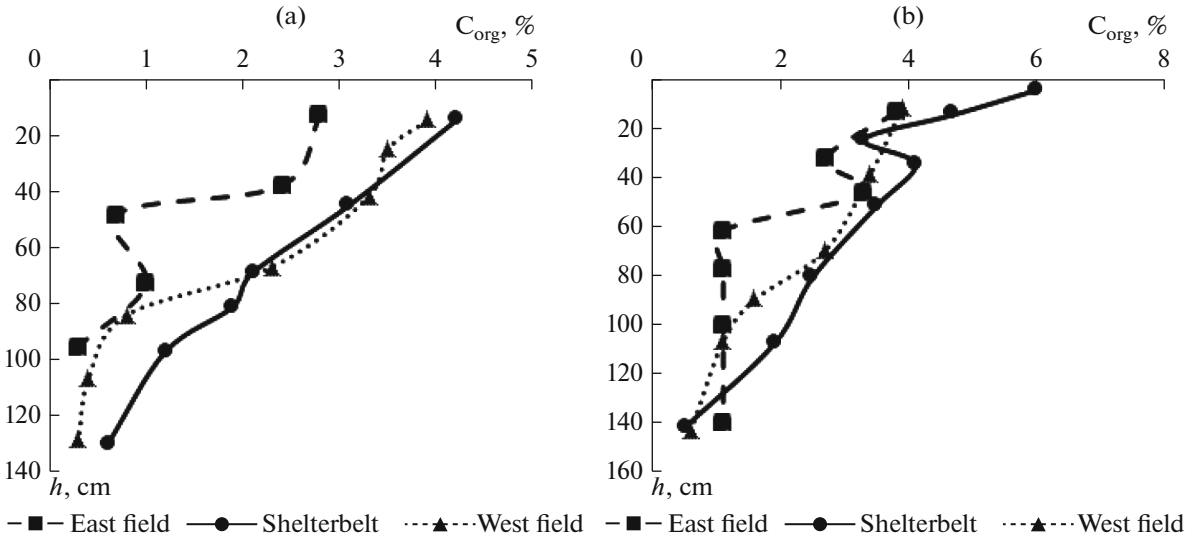

Fig. 5. The organic carbon content in soils of transects within the (a) watershed surface and (b) hollow bottom.

low-humus medium-deep-calcareous migrational–mycellar agrochernozem (Haplic Chernozem (Loamic, Aric, Pachic)) (profile 5E); medium-deep weakly humified deeply gleyic clay-illuvial agrochernozem on contrasting (two-layered) parent material (Luvic Stagnic Chernic Phaeozem (Loamic, Aric, Pachic, Raptic)) (profile 3W); deep weakly humified deep-calcareous deeply quasigleyic clay-illuvial agrochernozem on contrasting (two-layered) parent material (Luvic Stagnic Chernic Phaeozem (Loamic, Aric, Pachic)) (profile 8E); deep low-humus deep-calcareous clay-illuvial agrochernozem (Luvic Chernozem (Loamic, Aric, Pachic)) (profile 6S); deep weakly humified deep-calcareous clay-illuvial agrochernozem (Luvic Chernozem (Loamic, Aric, Pachic)) (profile 6W); medium-deep weakly humified medium-deep-calcareous clay-illuvial agrochernozem (Luvic Chernozem (Loamic, Aric, Pachic)) (profile 10S); medium-deep weakly humified deep-calcareous clay-illuvial agrochernozem (Luvic Chernozem (Loamic, Aric, Pachic)) (profile 6S); medium-deep weakly humified deep-calcareous clay-illuvial agrochernozem (Luvic Chernozem (Loamic, Aric, Pachic)) (profile 9S); deep low-humus deeply gleyic stratified eluviated clay-illuvial agrochernozem on contrasting parent material (Luvic Greyzemic Stagnic Chernic Phaeozem (Loamic, Aric, Novic, Pachic)) (profile 7S); and medium-deep medium-humus medium-deep-calcareous mycellar agrochernozem (Haplic Chernozem (Loamic, Aric, Pachic)) (profile 8S).

Let us consider the characteristics of the soils along the studied transects. Within the watershed surface, to which transect 9 is confined, the soils are represented by mycellar agrochernozems in the western and eastern fields (profiles 9W and 9E) and by clay-illuvial agrochernozems under the shelterbelt (profile 9S). The soils of the western and eastern fields on this transect slightly differ from one another. In both soils, their humus horizons are leached from carbonates; carbonate pedofeatures in the form of diffuse mottles and fine tubes (pseudomycelium) appear in the underlying transitional ABca horizon at a depth of 50 cm in profile 9E and 83 cm in profile 9W. In the underlying carbonate-accumulative BCA horizon, loose segregations of carbonates were diagnosed. Traces of periodic waterlogging were found in the form of rare olive and brownish rusty mottles (up to 1 cm in diameter) and iron–manganic concentrations. The thickness of the humus horizon and the content of organic carbon in the soils of profiles 9S and 9W are close (Fig. 5) and exceed those in the soil of profile 9E. The C_{org} content in the upper part of the humus horizon varies from 2.8 to 4.2%.

In the soil under the shelterbelt within the watershed transect 9, in contrast to the soils under the adjacent fields, the clay-illuvial BI horizon occurs under the humus horizon leached from carbonates at a depth of 70–115 cm. It is characterized by the presence of thin glossy films on ped faces having a darker color in comparison with the color of the intraped mass. Carbonate pedofeatures in the form of diffuse mottles and fine tubes are found from a depth of 115 cm in the BCA horizon. In the BI and BCA horizons, the features of periodic waterlogging were diagnosed in the form of rare and small olive and ocherous mottles (up to 1 mm in diameter) and iron-manganic concentrations. Thus, the main difference between the soils of the fields and the soil of the shelterbelt on the watershed surface within transect 9 is the presence of a clay-illuvial horizon in the soil under forest vegetation and its absence in the soils under agrocenoses. This feature may be due to the intensification of the illuviation of clay particles under woody vegetation in comparison with herbaceous vegetation of agrocenoses, as was shown in [2, 13].

Table 1. The values of taxonomic distances between soils

Indicator	Soils					
	watershed surface and gentle slopes	hollow bottom	steep slope	east field	shelterbelt	west field
Average values	1.06	0.38	1.22	1.37	0.99	1.22
Median values	1.41	0.57	1.31	1.47	1.28	1.41

A tendency for intensification of the clay-illuvial process in the soils under the shelterbelt, in comparison with the soils of the adjacent fields is also traced in other studied soils on the watershed surface (transects 2, 5) and on gentle slopes (transects 1, 10). Note that the formation of the BI horizon at the key site occurs not only in the soils of the shelterbelt, but also in some soils of the fields (for example, profiles 1W and 10W). However, the thickness of this horizon, and the integrity and thickness of clay coatings on ped faces in the soils under the shelterbelt are always higher than those in the soils of the adjacent fields. In general, the soils of the watershed surface and gentle slopes have the least contrast in relation to other soils of the key site (Table 1).

The soils of the bottom of the hollow (transect 7) are represented by stratified eluviated deep-gleyed clay-illuvial agrochernozems. A common feature of all three soils studied at this transect is the increased thickness of the plow horizon: 54 cm in profile 7E, 40 cm in profile 7S, and 55 cm in profile 7W. This can be due to the periodic accumulation of solid-phase matter carried by water flows from the overlying areas on the soil surface and the involvement of this material in the plowing process. A noticeably lower thickness of the old-arable horizon under the shelterbelt in comparison with plow horizons on the fields may be due to the erosion-control effect of the shelterbelt, which led to the accumulation of material on the soil surface in front of the shelterbelt and a decrease in the removal of material from the soil surface behind the shelterbelt. Under the humus horizon, in all the soils of the hollow, there is a transitional brown with a dark gray tint and a pronounced whitish powder along the edges of crumb–angular blocky aggregates in the ABel horizon. In the underlying BIel horizon, the whitish powder covers thin clay coatings. As in the case of the soils of the watershed and gentle slopes, the BIel horizon is more pronounced and thicker in the soil under the shelterbelt. In the soils of the adjacent fields, the lower part of the BDg horizon transitional to the parent material is characterized by clear indications of temporary waterlogging: bluish and ocherous mottles (gleyzation), thin bluish coatings of ped faces, and small iron–manganic concentrations are present in significant quantities. In the soil under the shelterbelt, the features of waterlogging are present only in the form of thin, intermittent bluish coatings and iron–manganic concentrations. All soils of transect 7 do not contain carbonates. The content of organic carbon has a surface-accumulative eluvial–illuvial pattern in the soil under the shelterbelt and under the eastern field and a clearly surface-accumulative pattern in the soil under the western field (Fig. 5b). Probably, this pattern of humus distribution reflects the additional accumulation of humus material in the bottom of the hollow. The humus content in the upper horizon varies from 3.9 to 6%. The soils of the bottom of the hollow have very high average and median values of taxonomic distances (Fig. 6), which indicates their high degree of difference from other soils of the key site. At the same time, the soils of the hollow themselves slightly differ from one another (Table 1)

Soils of steep slopes (slopes 4°–6°) are represented by clay-illuvial agrochernozems (profiles 6E, 3S, 6S, 4W, and 6W), including deep-gleyed soils (profiles 3E, 4S, and 3W), deep-quasigleyed soils (profile 8E), mycellar agrochernozems (profiles 8S and 8W), as well as by eluviated deep-gleyic agro-dark-humus soils (profile 4E). The latter soil is the most genetically unusual in comparison with other soils in the study area. In this soil, the soil profile is colored with humus color to a depth of 110 cm; the deep humus horizon is underlain by the yellowish-brown clay with bluishness. To a depth of 80 cm, the color of the soil is dark gray; deeper, it becomes whitish gray, and whitish powder appears on the edges of structural units; its amount increases down the soil profile. At a depth of 100–110 cm, the soil is characterized by a grayish-whitish color, with gray and brownish-yellow mottles. Judging the soil morphology, the following horizons were identified in this soil profile: PU (0–30 cm)–AU (30–80 cm)–AUel (80–100 cm)–ADel (100–110 cm) – Dg (110– 160 ... cm). The absence of an illuvial horizon in the presence of eluviation features in the AUel and ADel horizons in this soil may indicate the pronounced lateral gley-eluvial removal of soil products, which is favored by the contrasting composition of the two-layered parent material with the coarser (loamy) upper part underlain by the impermeable clayey stratum. This soil (profile 4E) is characterized by the largest average and median taxonomic distances (Fig. 6), which allows us to consider it the most different from all other studied soils of the key site.

In general, the calculation of taxonomic distances between soils under the eastern field, under the shelterbelt, and under the western field (i.e., in accordance with the soil grouping taking into account land use and the spatial position relative to the shelterbelt)

	1E	2E	3E	4E	5E	6E	7E	8E	9E	10E	1S	2S	3S	4S	5S	6S	7S	8S	9S	10S	1W	2W	3W	4W	5W	6W	7W	8W	9W	10W
1E	0.00	0.28	1.95	1.40	0.64	1.44	1.99	1.94	0.00	0.40	1.47	1.47	1.44	1.95	1.44	1.50	2.07	0.28	1.47	1.44	1.44	1.95	1.91	1.44	0.40	1.47	1.99	0.00	0.28	1.44
2E	0.28	0.00	1.93	1.43	0.57	1.47	2.01	1.96	0.28	0.28	1.44	1.44	1.41	1.93	1.41	1.47	2.05	0.28	1.47	1.44	1.41	1.93	1.93	1.41	0.28	1.50	2.01	0.28	0.00	1.41
3E	1.95	1.93	0.00	1.53	1.97	1.34	0.91	0.79	1.95	1.91	1.31	1.31	1.31	0.00	1.31	1.28	0.71	1.95	1.34	1.34	1.31	0.00	0.40	1.31	1.91	1.31	0.91	1.95	1.93	1.31
4E	1.40	1.43	1.53	0.00	1.49	1.99	1.58	1.67	1.40	1.40	2.01	2.01	2.01	1.53	2.01	1.99	1.53	1.43	2.01	2.01	2.01	1.53	1.53	2.01	1.40	1.97	1.58	1.40	1.43	2.01
5E	0.64	0.57	1.97	1.49	0.00	1.58	2.05	2.00	0.64	0.50	1.55	1.55	1.53	1.97	1.53	1.53	2.09	0.64	1.58	1.55	1.53	1.97	2.01	1.53	0.50	1.55	2.05	0.64	0.57	1.53
6E	1.44	1.47	1.34	1.99	1.58	0.00	1.40	1.29	1.44	1.50	0.28	0.28	0.40	1.34	0.40	0.40	1.51	1.47	0.28	0.40	0.40	1.34	1.28	0.40	1.50	0.28	1.40	1.44	1.47	0.40
7E	1.99	2.01	0.91	1.58	2.05	1.40	0.00	0.89	1.99	1.99	1.43	1.43	1.43	0.91	1.43	1.40	0.57	2.01	1.43	1.43	1.43	0.91	0.91	1.43	1.99	1.37	0.00	1.99	2.01	1.43
8E	1.94	1.96	0.79	1.67	2.00	1.29	0.89	0.00	1.94	1.94	1.32	1.32	1.35	0.79	1.35	1.29	1.06	1.96	1.32	1.35	1.35	0.79	0.79	1.35	1.94	1.26	0.89	1.94	1.96	1.35
9E	0.00	0.28	1.95	1.40	0.64	1.44	1.99	1.94	0.00	0.40	1.47	1.47	1.44	1.95	1.44	1.50	2.07	0.28	1.47	1.44	1.44	1.95	1.91	1.44	0.40	1.47	1.99	0.00	0.28	1.44
10E	0.40	0.28	1.91	1.40	0.50	1.50	1.99	1.94	0.40	0.00	1.47	1.47	1.44	1.91	1.44	1.44	2.03	0.40	1.50	1.47	1.44	1.91	1.95	1.44	0.00	1.47	1.99	0.40	0.28	1.44
1S	1.47	1.44	1.31	2.01	1.55	0.28	1.43	1.32	1.47	1.47	0.00	0.00	0.28	1.31	0.28	0.28	1.49	1.47	0.28	0.40	0.28	1.31	1.31	0.28	1.47	0.40	1.43	1.47	1.44	0.28
2S	1.47	1.44	1.31	2.01	1.55	0.28	1.43	1.32	1.47	1.47	0.00	0.00	0.28	1.31	0.28	0.28	1.49	1.47	0.28	0.40	0.28	1.31	1.31	0.28	1.47	0.40	1.43	1.47	1.44	0.28
3S	1.44	1.41	1.31	2.01	1.53	0.40	1.43	1.35	1.44	1.44	0.28	0.28	0.00	1.31	0.00	0.40	1.49	1.47	1.41	0.28	0.00	1.31	0.28	0.00	1.44	1.31	1.43	1.44	1.41	0.00
4S	1.95	1.93	0.00	1.53	1.97	1.34	0.91	0.79	1.95	1.91	1.31	1.31	1.31	0.00	1.31	1.28	0.71	1.95	1.34	1.34	1.31	0.00	0.40	1.31	1.91	1.31	0.91	1.95	1.93	1.31
5E	1.44	1.41	1.31	2.01	1.53	0.40	1.43	1.35	1.44	1.44	0.28	0.28	0.00	1.31	0.00	0.40	1.49	1.44	1.41	0.28	0.00	1.31	0.28	0.00	1.44	1.31	1.43	1.44	1.41	0.00
6S	1.50	1.47	1.28	1.99	1.53	0.40	1.40	1.29	1.50	1.44	0.28	0.28	0.40	1.28	0.40	0.00	1.46	1.50	0.40	0.49	0.40	1.28	1.34	0.40	1.44	0.28	1.40	1.50	1.47	0.40
7S	2.07	2.05	0.71	1.53	2.09	1.51	0.57	1.06	2.07	2.03	1.49	1.49	1.49	0.71	1.49	1.46	0.00	2.07	1.51	1.51	1.49	0.71	0.81	1.49	2.03	1.49	0.57	2.07	2.05	1.49
8S	0.28	0.28	1.95	1.43	0.64	1.47	2.01	1.96	0.28	0.40	1.47	1.47	1.47	1.95	1.44	1.50	2.07	0.00	1.44	1.41	1.44	1.95	1.93	1.44	0.40	1.50	2.01	0.28	0.28	1.44
9S	1.47	1.47	1.34	2.01	1.58	0.28	1.43	1.32	1.47	1.50	0.28	0.28	1.41	1.34	1.41	0.40	1.51	1.44	0.00	1.44	1.41	1.34	1.41	1.41	1.50	1.92	1.43	1.47	1.47	1.41
10S	1.44	1.44	1.34	2.01	1.55	0.40	1.43	1.35	1.44	1.47	0.40	0.40	0.28	1.34	0.28	0.49	1.51	1.41	1.44	0.00	0.28	1.34	0.40	0.28	1.47	1.31	1.43	1.44	1.44	0.28
1W	1.44	1.41	1.31	2.01	1.53	0.40	1.43	1.35	1.44	1.44	0.28	0.28	0.00	1.31	0.00	0.40	1.49	1.44	1.41	0.28	0.00	1.31	0.28	0.00	1.44	1.31	1.43	1.44	1.41	0.00
2W	1.95	1.93	0.00	1.53	1.97	1.34	0.91	0.79	1.95	1.91	1.31	1.31	1.31	0.00	1.31	1.28	0.71	1.95	1.34	1.34	1.31	0.00	0.40	1.31	1.91	1.31	0.91	1.95	1.93	1.31
3W	1.91	1.93	0.40	1.53	2.01	1.28	0.91	0.79	1.91	1.95	1.31	1.31	0.28	0.40	0.28	1.34	0.81	1.93	1.41	0.40	0.28	0.40	0.00	0.28	1.95	1.31	0.91	1.91	1.93	0.28
4W	1.44	1.41	1.31	2.01	1.53	0.40	1.43	1.35	1.44	1.44	0.28	0.28	0.00	1.31	0.00	0.40	1.49	1.44	1.41	0.28	0.00	1.31	0.28	0.00	1.44	1.31	1.43	1.44	1.41	0.00
5W	0.40	0.28	1.91	1.40	0.50	1.50	1.99	1.94	0.40	0.00	1.47	1.47	1.44	1.91	1.44	1.44	2.03	0.40	1.50	1.47	1.44	1.91	1.95	1.44	0.00	1.47	1.99	0.40	0.28	1.44
6W	1.47	1.50	1.31	1.97	1.55	0.28	1.37	1.26	1.47	1.47	0.40	0.40	1.31	1.31	1.31	0.28	1.49	1.50	1.92	1.31	1.31	1.31	1.31	1.31	1.47	0.00	1.37	1.47	1.50	1.31
7W	1.99	2.01	0.91	1.58	2.05	1.40	0.00	0.89	1.99	1.99	1.43	1.43	1.43	0.91	1.43	1.40	0.57	2.01	1.43	1.43	1.43	0.91	0.91	1.43	1.99	1.37	0.00	1.99	2.01	1.43
8W	0.00	0.28	1.95	1.40	0.64	1.44	1.99	1.94	0.00	0.40	1.47	1.47	1.44	1.95	1.44	1.50	2.07	0.28	1.47	1.44	1.44	1.95	1.91	1.44	0.40	1.47	1.99	0.00	0.28	1.44
9W	0.28	0.00	1.93	1.43	0.57	1.47	2.01	1.96	0.28	0.28	1.44	1.44	1.41	1.93	1.41	1.47	2.05	0.28	1.47	1.44	1.41	1.93	1.93	1.41	0.28	1.50	2.01	0.28	0.00	1.41
10W	1.44	1.41	1.31	2.01	1.53	0.40	1.43	1.35	1.44	1.44	0.28	0.28	0.00	1.31	0.00	0.40	1.49	1.44	1.41	0.28	0.00	1.31	0.28	0.00	1.44	1.31	1.43	1.44	1.41	0.00
Average	1.23	1.22	1.28	1.64	1.36	1.00	1.39	1.37	1.23	1.24	0.97	0.97	0.98	1.28	0.98	1.01	1.44	1.25	1.27	1.04	0.98	1.28	1.11	0.98	1.24	1.24	1.39	1.23	1.22	0.98
Median	1.44	1.44	1.31	1.55	1.53	1.34	1.43	1.35	1.44	1.44	1.31	1.31	1.33	1.31	1.33	1.28	1.49	1.44	1.42	1.35	1.33	1.31	1.29	1.33	1.44	1.31	1.43	1.44	1.44	1.33
Maximum	2.07	2.05	1.97	2.01	2.09	1.99	2.05	2.00	2.07	2.03	2.01	2.01	2.01	1.97	2.01	1.99	2.09	2.07	2.01	2.01	2.01	1.97	2.01	2.01	2.03	1.97	2.05	2.07	2.05	2.01

Fig. 6. Taxonomic distances between soils of the key site. The intensity of shading reflects the grade of taxonomic distance (darker shading corresponds to higher taxonomic distances). 1E, 2E, 3E... are the numbers of soil pits.

Table 2. Properties of soils of the shelterbelt and adjacent fields

Soil location	Average value	Median value	Minimum	Maximum	Range
Thickness of the humus horizon, cm					
East field	49.5	50	32	65	33
Shelterbelt	60.8	60	30	60	30
West field	55	60	28	72	44
Thickness of the humus profile, cm					
East field	71.0	70.0	50	100	50
Shelterbelt	72.5	75.0	55	100	45
West field	70.8	71.0	40	100	60
Organic carbon content, %					
East field	3.86	3.65	2.8	4.9	2.1
Shelterbelt	4.73	4.65	4	5.9	1.9
West field	3.99	4.1	2.9	4.5	1.6
Depth of effervescence with 10% HCl					
East field	68.7	51.0	40.0	120.0	80.0
Shelterbelt	78.1	75.0	60.0	115.0	55.0
West field	67.9	60.0	50.0	100.0	50.0
Depth of secondary carbonate concentrations in soil profiles					
East field	68.7	51.0	40.0	120.0	80.0
Shelterbelt	78.1	75	60.0	115.0	55.0
West field	67.9	60	50	100.0	50
Content of the CO_2 of carbonates in effervescing horizons, %					
East field	2.2	2.1	1.0	4.4	3.4
Shelterbelt	2.5	1.8	0.7	5.7	5.0
West field	3.0	2.5	1.0	6.6	5.6
Content of the CO_2 of carbonates in the horizon containing carbonate concentrations, %					
East field	3.0	3.4	1.0	5.3	4.3
Shelterbelt	3.3	3.7	0.7	5.7	5.0
West field	4.2	4.1	1.2	6.6	5.4

with 10 soils in each sample shows that the soils under the shelterbelt are the least contrasting in relation to one another in comparison with the soils under the adjacent fields. In this case, the maximum contrast in relation to one another is characteristic of the soils of the eastern field, in terms of both the average and the median values of taxonomic distances (Table 1).

Figure 2 displays the soil map of the key site, for which soils were diagnosed at the subtype level. The largest area is occupied by mycellar agrochernozems; then, in decreasing order, there area deep-gleyed clay-illuvial agrochernozems, stratified eluviated deep-gley clay-illuvial agrochernozems, migrational–mycellar agrochernozems, deep-quasigleyed clay-illuvial agrochernozems, and eluviated deeply gleyic agro-dark-humus soils. The maximum number of components with which the given soil areas have common boundary (the number of neighbors) is equal to three, and it is observed for the areas of stratified eluviated deep-gleyic clay-illuvial agrochernozems and for the area of the mycellar agrochernozem. On average, soil areas have common boundary with two neighbors. We assume that the soil cover pattern of the key site can be defined as low-contrasting microcombinations of mycellar, migrational–mycellar, and clay-illuvial agrochernozems on the watershed surface; disordered striated low-contrasting mesocombinations of migrational–mycellar and clay-illuvial agrochernozems (including deeply gleyic and deeply quasigleyic variants) of the water-migratory and, to a lesser extent, erosional genesis on slopes; there are also more contrasting combinations of deeply gleyic clay-illuvial agrochernozems and deeply gleyic eluviated agro-dark-humus soils.

If we pay attention to the particular soil properties (Table 2, Fig. 2), we can see that the soils formed under the shelterbelt have the smallest scattering of values of the thickness of the humus horizon, the thickness of the entire humus profile, and the organic carbon content. For these soils, in general (if we do not take into account the soils formed in positions of a shallow embedding by the carbonate-free clay), the level of effervescence is found deeper than in the soils of the adjacent fields; the depth of carbonate pedofeatures is also deeper under the shelterbelt. This observation is also confirmed by other studies of changes in the carbonate profile of chernozems under the impact of forest vegetation [2, 17]. The greatest scattering of

Table 3. The values of pedodiversity indices

Index	East field	Shelterbelt	West field
Richness	9	8	8
Shannon	1.60	0.89	1.42
Simpson	0.87	0.83	0.86
Rao	0.60	0.42	0.54

the values of these indicators is characteristic of the soils of the eastern field. Apparently, these soils are developed under the most contrasting moistening conditions. Naturally, in the direction from the soils of the eastern field to the soils under the shelterbelt and to the soils of the western field (which follows the general slope of the surface towards the west), an increase in the content of carbonates takes place in the horizon with effervescence, but without carbonate concentrations, as well as in the deeper horizon with distinct carbonate concentrations (pedofeatures).

Table 3 shows the values of the diversity indices; Among the factors that determine the spatial diversity of soils at the key site, an important role is played by the heterogeneity of parent material with local outcropping of the layer of carbonate-free clay to the surface and by the forest shelterbelt. The two-layered structure of parent material was diagnosed in four profiles studied on the eastern field, three profiles studied on the western field, and two profiles studied under the shelterbelt. Trees act as a physical barrier that retains snow and takes up moisture from the deep horizons with its further transpiration. In general, the microclimatic conditions under the tree canopy differ from those on the adjacent fields and affect the surface and soil runoff processes. In particular, the shelterbelt contributes to seasonal waterlogging of soils of the eastern field within the hollow (Fig. 3). As a result of the superposition of these factors, the area adjacent to the shelterbelt from the east is characterized by slightly higher quantitative indicators of pedodiversity (Table 3). The values of the Shannon, Simpson, and Rao indices (Table 3) calculated for the eastern and western fields vary within the limits of 1.42–1.6, 0.86–0.87, and 0.54–0.6, respectively. We assume that, before forest reclamation, the values of the diversity indices for the soils, which are now under the shelterbelt, were approximately within the same intervals. However, at present, under the shelterbelt of 50–55 years in age, they are significantly lower. Thus, the comparison of diversity indices (Table 3) and average and median values of taxonomic distances (Table 1) attest to a decrease in the spatial diversity of soils and the degree of contrast between them under the shelterbelt in comparison with soils of the adjacent fields.

CONCLUSIONS

The study of the soils under the shelterbelt and on the adjacent agricultural fields attests to considerable influence of the long-term-functioning of forest plantations in the agrolandscapes of the forest-steppe zone on the local pedodiversity made it possible to formulate the following conclusions:

(a) Field-protective afforestation over a half-century period leads to a decrease in the degree of contrast of soils in relation to one another directly under the shelterbelt;

(b) The soils under the shelterbelt, in comparison with the soils of the adjacent fields, are characterized by the smallest ranges of values of the thickness of their humus horizon and the entire humus profile and of the organic carbon content; and

(c) Lower values of the Shannon, Simpson, and Rao diversity for the soil cover under the shelterbelt are observed against the background of higher and similar values of these indices for the soils of adjacent fields, which may indicate a decrease in the spatial diversity of soils under the impact of afforestation (planting of the shelterbelt).

ACKNOWLEDGMENTS

The authors are deeply grateful to N.B. Khitrov for discussing the research results, making comments and suggestions.

FUNDING

This study was supported by the Russian Science Foundation, project no. 19-17-00056.

CONFLICT OF INTEREST

The authors declare that they have no conflict of interest.

REFERENCES

1. *Agroecological State of Chernozems in the Central Chernozemic Region*, Ed. by A. P. Shcherbakov and I. I. Vasenev (Kursk, 1996) [in Russian].
2. A. L. Aleksandrovskii, "Models of pedolithogenesis and soil evolution," in *Proceedings of VIII International Scientific Conference "Problems of Nature Management*

and Ecological Situation in European Russia and Adjacent Territories," Belgorod, October 22–25, 2019 (Belgorod State University, Belgorod, 2019), pp. 23–30.

3. I. O. Alyabina, "Cartographic assessment of soil diversity in Russia," Moscow Univ. Soil Sci. Bull. **73**, 5–10 (2018).
4. V. I. Erusalimskii and V. A. Rozhkov, "Multifunctional role of protective forest plantations," Byull. Pochv. Inst. im. V.V. Dokuchaeva, No. 88, 121–137 (2017).
5. E. A. Zazdravnykh, Candidate's Dissertation in Geography (Belgorod State University, Belgorod, 2017) [in Russian].
6. L. L. Shishov, V. D. Tonkonogov, I. I. Lebedeva, and M. I. Gerasimova, *Classification and Diagnostic System of Russian Soils* (Oikumena, Smolensk, 2004) [in Russian].
7. P. V. Krasilnikov, M. I. Gerasimova, D. L. Golovanov, M. V. Konyushkova, V. A. Sidorova, and A. S. Sorokin, "Pedodiversity and its significance in the context of modern soil geography," Eurasian Soil Sci. **51**, 1–13 (2018). https://doi.org/10.1134/S1064229318010118
8. V. M. Kretinin, "Monitoring of soil fertility in agroforest landscapes of the forest-steppe zone," Dokl. Vses. Akad. S-kh. Nauk im. V.I. Lenina, No. **3**, 16–20 (1992).
9. M. A. Smirnova and M. I. Gerasimova, "Orders in the soil classification system of Russia: Taxonomic distance as a measure of their adequate identification," Eurasian Soil Sci. **50**, 263–275 (2017). https://doi.org/10.1134/S1064229317030115
10. A. V. Stetsenko, Possibilities to control negative changes in agriculture using economic mechanisms mentioned in the Kyoto Protocol, 2011. http://kyotoforests.narod.ru.
11. N. B. Khitrov, "The development of detailed soil maps on the basis of interpolation of data on soil properties," Eurasian Soil Sci. **45**, 918–928 (2012).
12. N. D. Chegodaeva, I. F. Kargin, and V. I. Astradamov, *Effect of Forest Shelterbelts on Soil Water-Physical Properties and Ground Beetles Population on Adjacent Field* (Mordovsk. Knizhn. Izd., Saransk, 2005) [in Russian].
13. Yu. G. Chendev and V. P. Kriushin, "Spatiotemporal changes of some chernozems in the East European Plain," Izv. Ross. Akad. Nauk, Ser. Geogr., No. 1, 73–82 (2007).
14. D. I. Shcheglov, *Chernozems of the Center of the Russian Plain and Their Evolution under the Impact of Natural and Anthropogenic Factors* (Nauka, Moscow, 1999) [in Russian].
15. J. G. Bockheim and S. A. Schliemann, "Soil richness and endemism across an environmental transition zone in Wisconsin, USA," Catena **113**, 86–94 (2014). https://doi.org/10.1016/j.catena.2013.09.011
16. J. R. Brandle, L. Hodges, and X. H. Zhou, "Windbreaks in North American agricultural systems," Agrofor. Syst. **61**, 65–78 (2004).
17. Yu. Chendev, A. Gennadiev, T. Sauer, E. Terekhin, and S. Matveev, "Forests advancements to grasslands and their influence on soil formation: forest steppe of the Central Russian Upland," IOP Conf. Ser.: Earth Environ. Sci. **392**, 012003 (2019). https://doi.org/10.1088/1755-1315/392/1/012003
18. E. A. C. Costantini and G. L'Abate, "The soil cultural heritage of Italy: Geodatabase, maps, and pedodiversity evaluation," Quat. Int. **209** (1–2), 142–153 (2009). https://doi.org/10.1016/j.quaint.2009.02.028
19. T. Fu, L. Han, H. Gao, H. Liang, and J. Liu, "Geostatistical analysis of pedodiversity in Taihang Mountain region in North China," Geoderma **11** (32), 91–99 (2017). https://doi.org/10.1016/j.geoderma.2018.05.010
20. J. J. Ibáñez, R. J. Vargas, and A. Vázquez-Hoehne, "Pedodiversity state of the art and future challenges," in *Pedodiversity* (CRC Press, Boca Raton, FL, 2013), pp. 1–28. https://doi.org/10.1201/b14780-2
21. J. Kort, "Benefits of windbreaks to field and forage crops," Agric. Ecosyst. Environ. **22–23**, 165–190 (1988). https://doi.org/10.1016/b978-0-444-43019-9.50018-3
22. B. Minasny and A. B. McBratney, "Incorporating taxonomic distance into spatial prediction and digital mapping of soil classes," Geoderma **142**, 285–293 (2007). https://doi.org/10.1016/j.geoderma.2007.08.022
23. B. Minasny, A. B. McBratney, and A. E. Hartemink, "Global pedodiversity, taxonomic distance, and the World Reference Base," Geoderma **155**, 132–139 (2010). https://doi.org/10.1016/j.geoderma.2009.04.024
24. C. H. Perry, C. W. Woodall, G. C. Liknes, and M. M. Schoeneberger, "Filling the gap: improving estimates of working tree resources in agricultural landscapes," Agrofor. Syst. **75** (1), 91–101 (2009). https://doi.org/10.1007/s10457-008-9125-6
25. A. Petersen, A. Grongroft, and G. Miehlich, "Methods to quantify the pedodiversity of 1 km^2 areas—results from southern African drylands," Geoderma **155** (3–4), 140–146 (2009). https://doi.org/10.1016/j.geoderma.2009.07.009
26. C. R. Rao, "Diversity and dissimilarity coefficients: a unified approach," Theor. Popul. Biol. **21** (1), 24–43 (1982). doi 1016/0040-5809(82)90004-1
27. N. Toomanian and I. Esfandiarpoor, "Challenges of pedodiversity in soil science," Eurasian Soil Sci. **43**, 1486–1502 (2010). https://doi.org/10.1134/S1064229310130089

Translated by D. Konyushkov